energy&fuels

pubs.acs.org/EF Article

Insight into Polyethylene and Polypropylene Pyrolysis: Global and Mechanistic Models

Rebecca E. Harmon, Gorugantu SriBala, Linda J. Broadbelt, and Alan K. Burnham*

Cite This: *Energy Fuels* 2021, 35, 6765–6775 Read Online

ACCESS | Metrics & More | Article Recommendations

ABSTRACT: Pyrolysis of polyolefins has been proposed as a potential resource recovery strategy by converting macromolecules into valuable fuels and chemicals. Due to variations in possible backbone structures, chain-length distributions, and arrangements of pendant groups, their decomposition behavior via pyrolysis can be complex. In the present work, a review of historical data and empirical models for two distinct polyolefins, polyethylene (PE) and polypropylene (PP), is provided followed by a comparison to recent mechanistic models. The characteristic sigmoidal behavior of linear polymer decomposition is captured with global, lumped-species, and mechanistic models of high-density polyethylene. The PE model was extended to simulate PP using the same reaction families and reaction family parameters, but with distinct rate coefficients that accounted for the difference in the structure of PP with its pendant methyl groups compared to PE as manifested through heats of reaction embedded in the Evans–Polanyi relationship, $E_a = E_0 + \gamma \times \Delta H_{reacn}$. The change in structure and its associated kinetic parameters resulted in no sigmoidal conversion, consistent with experimental reports for atactic PP. This suggests that mechanistic modeling could be an important complement to global model studies to understand when other effects are at play in the pyrolytic decomposition of polymers such as PP.

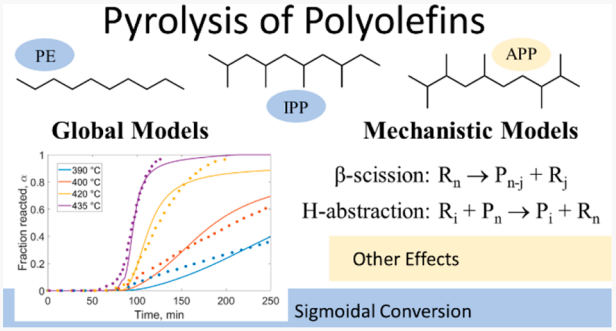

INTRODUCTION

Hydrocarbon polymers are now a pervasive product of our industrial age to the point that they are a significant environmental pollution problem. Although there are active efforts to increase recycling in the polymer form, they are also a potential source of energy in general and liquid fuels, in particular due to their favorable molecular structure. For example, single-use plastics can be converted to naphtha, opening an avenue to integrate plastics as a feedstock in petroleum refineries.[1] Liquid fuels have a higher value per weight than when used either by combustion in raw form or after conversion to syngas. Some have even proposed mini-pyrolysis units to generate fuel oil locally for cooking stoves in developing parts of the world.[2] This use could have beneficial environmental and health benefits as long as halogenated polymers were excluded.

In addition, oil and gas are formed in the subsurface by pyrolysis reactions that occur over millions of years. While this is not a typical perception of pyrolysis conditions, petroleum geochemists have developed chemical reaction models for these reactions based on laboratory pyrolysis experiments. Some well-preserved algal kerogens have linear structures that give sigmoidal conversion character similar to that of linear polymers,[3] while others have branched and cross-linked structures that require distributed reaction models.[4] Also, understanding how secondary reactions change as a function of time, temperature, and pressure can help understand the reliability of petroleum generation and cracking reactions.[5]

Conversion of polymers to any new product requires an understanding of how time, temperature, and pressure affect the product distribution and quality as a function of molecular structure, including weak links, branching, and crystallinity. Included in this goal is understanding how compositional variations in the feedstock affect the conditions for optimum product quality and value. The current work is motivated to address that issue. It also follows in the spirit of our previous contribution addressing cellulose pyrolysis.[6]

Process modeling has historically taken various approaches, which might be described approximately in terms of three classes: global kinetic models, lumped-species pseudomechanistic models, and true mechanistic models.[7] In this work, we first review the experimental data from literature for polyethylene (PE) and polypropylene (PP), which are two very common commodity polymers, and later explore connections

Received: January 30, 2021
Revised: March 24, 2021
Published: April 2, 2021

https://doi.org/10.1021/acs.energyfuels.1c00342
Energy Fuels 2021, 35, 6765–6775

and discrepancies among those three approaches for the thermal degradation of polymers.

LUMPED-SPECIES AND GLOBAL KINETICS MODELS

True mechanistic models for polymer pyrolysis contain hundreds of species and thousands of reactions. In lumped-species models, the mechanism is reduced to several species and perhaps a dozen reactions, depending on the material and application. Global kinetic models further simplify the reaction network to one or two reactions with a global stoichiometric product distribution. Mechanistic details are lost through this progressive simplification, but if done well, the resulting models capture the most important aspects of the reaction mechanism.

Polyolefin polymers decompose by a free-radical chain reaction mechanism. The fundamentals of free-radical chain reactions date back to Rice and co-workers[8,9] at about the same time that PE started being produced commercially. Excellent work on thermal decomposition of polyolefins was conducted in the 1940s and 1950s, much of which was reported in 1953 in the National Bureau of Standards Circular 525.[10] Kinetic concepts first presented in that document are applied in this work. Specifically, the reaction may be either deceleratory or sigmoidal, depending on the polymeric structure and the details of its decomposition mechanism. By deceleratory, we mean that the rate of decomposition is at its maximum value at the initial time for isothermal conditions. In contrast, a sigmoidal reaction profile starts with a small rate at the initial time and then rises to a maximum rate before declining to zero as the material is consumed.

The overall decomposition of a long hydrocarbon chain, be it in petroleum or a polymer, is described generally by

end initiation:	$P_n \rightarrow R_{n-1} + R_1$
random initiation:	$P_n \rightarrow R_{n-i} + R_i$
hydrogen abstraction:	$R_i + P_n \rightarrow P_i + R_n$
β-scission:	$R_n \rightarrow P_{n-j} + R_j$
depropagation:	$R_n \rightarrow R_{n-1} + P_1$
termination by disproportionation:	$R_i + R_j \rightarrow P_i + P_j$
termination by recombination:	$R_i + R_j \rightarrow P_{i+j}$

where P_i is a dead polymer chain of length i and R_j is a radical of length j. Here, depropagation is listed as a separate reaction from β-scission to show explicitly the formation of monomers, but it is rigorously a β-scission reaction. Furthermore, in more detailed mechanistic treatments of polymer pyrolysis developed by Broadbelt and co-workers,[11−14] the reverse of β-scission, i.e., radical addition, is also included, and backbiting reactions such as 1,5- and 1,4-hydrogen transfer are also incorporated.

There are some variations in this formalism in the literature. For example, Simha and Wall[15] do not consider termination by recombination, and Bouster et al.[16] do not distinguish between random and end initiation. In the most detailed mechanistic treatments currently available, however, the highest degree of detail possible is maintained so that reactivity and structure are explicitly linked.[11,12,14] Because mechanistic models can be challenging to develop and solve, various simplifications have been invoked. For example, Simha and Wall used their limited mechanism to develop statistical models on how molecular weight evolves with time. Starting with an initial chain length of N and picking a threshold chain length, L, for volatilization, they obtained

$$1 - \alpha = (1 - x)^{L-1}\left[\frac{(N - L)(L - 1)}{N}\right] \quad (1)$$

where x is the fraction of bonds broken and α is the fraction volatilized. Burnham et al.[3] used qualitative arguments to draw links among this equation, the Prout−Tompkins equation,[17] and its extended form with a non-integer growth coefficient.[18] Further, Sanchez-Jimenez et al.[19] derived a more rigorous relationship between α and x:

$$d\alpha/dt = kL(L - 1)\, x(1 - x)^{L-1} \quad (2)$$

where k is the reaction rate constant. In the conventional notation of thermal analysis, the reaction rate is usually expressed as a rate constant times a simple function of conversion ($d\alpha/dt = kf(\alpha)$), so

$$f(\alpha) = L(L - 1)\, x(1 - x)^{L-1} \quad (3)$$

For $L = 2$, this equation is the standard logistic (Prout−Tompkins) model. The shape of a plot of $f(\alpha)$ versus α is approximately independent of L, but the overall reaction rate increases, because fewer bonds must be broken to form a volatile fragment. If the reactivity of the remaining material were the same as the original, $f(\alpha)$ would equal $1 - \alpha$, a first-order reaction, so the amount of deviation from first order is a measure of the change in reactivity of the remaining material.

Bouster et al.[16] approach the solution a little differently and derive the relation (again, in thermal analysis notation):

$$f(\alpha) = (1 - \alpha)[1 - (1 - \alpha)^{2b}]^{1/2} \quad (4)$$

where b for polypropylene[20] also has an Arrhenius form, $b = b_o \exp(-E_b/RT)$.

Out of the solid-state decomposition literature comes the JMAEK[21−24] and Prout−Tompkins[17] models, and the following briefly summarizes the description presented earlier for cellulose pyrolysis.[6] The JMAEK model is a random nucleation and geometric growth model in which the reaction rate increases with the growing reaction interface but eventually declines as the reaction volumes converge. In thermal analysis formalism, it is given by

$$f(\alpha) = p(1 - \alpha)[-\ln(1 - \alpha)]^{(p-1)/p} \quad (5)$$

where p is a growth dimensionality. The Prout−Tompkins model is simply the empirical application of the standard logistic equation to sigmoidal reactions. It has been used with both linear and logarithmic time. More interesting, it can be related to a first-order autocatalytic reaction which, after generalization and simplification, gives the extended Prout−Tompkins (ePT) equation[18]

$$f(\alpha) = (1 - \alpha)^n[1 - q(1 - \alpha)]^m \quad (6)$$

where n is a reaction order and m is a growth coefficient that is approximately equal to $p - 1$ for similar reaction profiles. The parameter q approximately equals $1 - k_1/k_2$, where k_1 is the rate coefficient for the initiation (nucleation) reaction, and k_2 is the rate coefficient for the propagation (growth) reaction.[25] The ratio k_2/k_1 is called the autocatalytic strength and

https://doi.org/10.1021/acs.energyfuels.1c00342
Energy Fuels 2021, 35, 6765−6775

correlates with the tendency of the reaction to run away if it is exothermic and combined with poor heat dissipation.

GLOBAL KINETICS ANALYSIS OF POLYETHYLENE DECOMPOSITION

Chemical kinetic studies of PE have a long history, with the most extensive work being in the 1950s at the National Bureau of Standards and reviewed by Flynn and Florin.[26] These early isothermal studies established that linear PE had a maximum reaction rate at 20−40% conversion, with the latter being at the highest temperature, 420 °C. However, these experiments were conducted in a vacuum, which enhances volatilization, so caution is warranted when applying these conclusions to relatively rapid heating rates at atmospheric pressure.

Westerhout et al.[27] reviewed the literature and commented that most workers inappropriately use a simple *n*th-order reaction. Their data in N_2 at atmospheric pressure confirm the NBS results that a maximum volatilization rate occurs at about 30% conversion for isothermal heating of high-density (linear) PE, which requires some sort of sigmoidal reaction model.

Rates of thermal decomposition of an unspecified high-density polyethylene (HDPE)[28] were obtained in 1996 using a Pyromat instrument[4] with a flame ionization detector. Replicates were run at heating rates of 0.97 and 50.5 °C/min to ensure precision, and a single run at 6.8 °C/min verified the interpolation of the reaction profile shape. Those data were fitted to the ePT model using q = 0.99, and the results are shown in Table 1 and Figure 1. The extended Kissinger method[18] uses profile width and asymmetry to estimate m and n and an adjusted value of A for the ePT model, and those values were used as initial conditions for the nonlinear optimization on measured reaction rates. Allowing n to be optimized enabled a significantly better fit due to the asymmetry of the reaction profile. The activation energies are in the middle of the range reported in the literature.[29]

Although there is no universally accepted method of calculating uncertainties from nonlinear regression as exists for linear regression, comments about the uncertainty in A and E_a are appropriate. First, the standard error in E_a from Kissinger's analysis is only ±0.2 kJ/mol, and the corresponding correlated change in A is 3%. These values represent the statistical uncertainly only and not the effects of any systematic errors, such as a nonconstant error in temperature calibration as a function of temperature, so the true error is larger by some unknown factor. For nonlinear regression, the uncertainties of all four fitted parameters are correlated. Constraining E_a to 246.6 kJ/mol increases the r.s.s. of rates by 0.1% and decreases the r.s.s. of conversion by 4.5%. This result points out an additional uncertainty aspect that the regression results will depend on whether one optimizes on reaction rates, conversion, or a combination of both. For the purposes of this work, there is certainly no significant difference in the three E_a values in Table 1.

Scaled master plots have been a standard way of examining kinetic models for decades. Recently, Gotor et al.[30] presented various methods that can be applied to both isothermal and ramped heating experiments. The most useful method in terms of being able to discriminate various mechanisms is

$$\frac{f(\alpha)}{f(0.5)} = \frac{d\alpha/dt}{d\alpha/dt_{\alpha=0.5}} \frac{\exp(E_a/RT)}{\exp(E_a/RT_{0.5})} \quad (7)$$

where the reaction rates are normalized at half-conversion and scaled for arbitrary thermal histories by the apparent activation energy.

The normalized reaction rate plot calculated using eq 7 is shown in Figure 2. The calculated curve used the parameters in Table 1 that were optimized for n. The experimental maxima are at about 30% conversion at 0.97 °C/min (lower reaction temperature) and 40% at 50.5 °C/min (higher reaction temperature). This trend is the same as that observed by

Table 1. Extended Prout−Tompkins Kinetic Parameters for HDPE

param	extended Kissinger	n constrained	n optimized
A, s^{-1}	1.965×10^{15}	1.886×10^{15}	1.715×10^{15}
E_a, kJ/mol	246.4	246.3	247.0
m	0.64	0.562	0.464
n	0.94	1.00	0.824
r.s.s. of rates[a]		2.04	1.59
r.s.s. of conversion[b]		0.463	0.353

[a]Sum of squares of normalized rate residuals. [b]Sum of squares of normalized cumulative residuals.

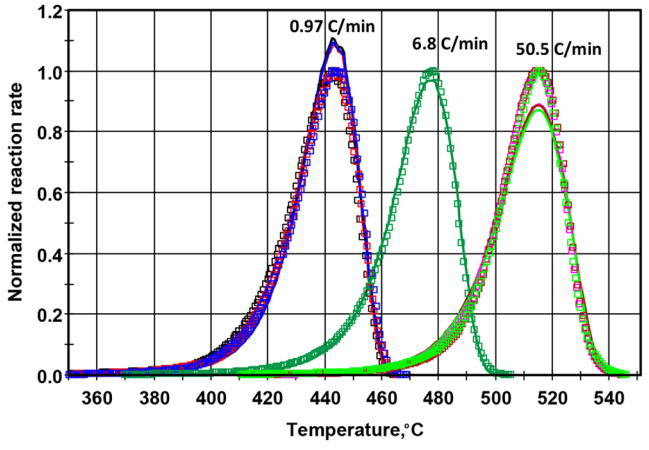

Figure 1. Comparison of measured[28] (shown as points) and calculated (shown as lines) reaction rates with repeated runs at 0.97 and 50.5 °C/min heating rates for thermal decomposition of HDPE using parameters optimized, including reaction order.

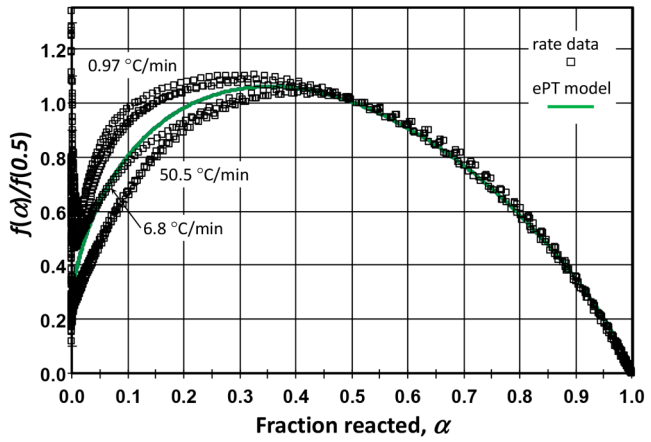

Figure 2. Normalized reaction rate plot for HPDE at three different heating rates, 0.97, 6.8, and 50.5 °C/min. The 0.97 and 50.5 °C/min lines cluster above and below the calculated curve, respectively.

https://doi.org/10.1021/acs.energyfuels.1c00342
Energy Fuels 2021, 35, 6765−6775

Bouster et al.[16] for polystyrene and PP. A related breakdown of a single activation energy model is reflected in the reaction profiles becoming narrower in Figure 1 relative to the ePT model as the heating rate increases. This result indicates that the temperature dependence is more complex than can be modeled by a single activation energy model, so caution should be used when extrapolating outside the range of calibration. Even though the maximum rate occurs at different conversions for isothermal conditions, it occurs at 64% conversion at all heating rates, with an overall standard error of 1.5%. Consequently, even though Kissinger's method is known to breakdown sometimes,[31] that does not appear to be the case here.

Polyethylene decomposition kinetics vary due to the amount of branching and possibly other factors. The degree of branching affects the number of secondary and tertiary carbon atoms, but it is also reflected in the density and crystallinity. More chain linearity and fewer weak links lead to a narrower reaction profile. Of course, the reaction profile can also be affected by additives and heat and mass transfer effects, so comparison with literature data must be interpreted cautiously.

A survey of the literature indicates that the LLNL Pyromat reaction profiles in Figure 1 and in Burnham and Braun[28] are narrower than most others in the literature. Specifically, the ΔT between 10 and 90% conversion are 37 and 34 °C, respectively, for low-density polyethylene (LDPE) and HDPE. These values are compared in Figure 3 to profile widths estimated from published reaction profiles[29,32−39] as a function of T_{max} at 10 °C/min for 15 determinations in addition to the Pyromat measurements. The HDPE samples tend to have higher T_{max} values and narrower profile widths, although there is considerable scatter due to digitization and calibration issues. For the five cases in which one laboratory studied both materials, the T_{max} values averaged 4 °C higher, and profile widths averaged 6 °C narrower for HDPE. Obviously, a much better relationship could be determined by a single laboratory measuring a set of samples having a range of densities.

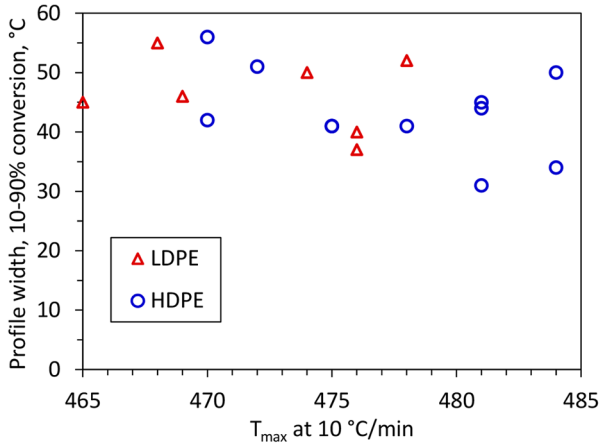

Figure 3. Plot of pyrolysis reaction profile widths[29,32−39] as a function of the temperature of maximum reaction when LDPE or HDPE is heated at 10 °C/min.

The 20 °C temperature range of T_{max} in Figure 3 indicates a large variation in reactivity for different polyethylene samples. Even allowing that 5−10 °C of that range is due to temperature calibration errors and variations in peak shape, the remaining 10−15 °C range is substantial. For a typical E_a value of 245 kJ/mol, every 5 °C shift corresponds to a change in the reaction rate of 30%. A plausibly real range of 15 °C in T_{max} implies a 2.3× variation in the time required to pyrolyze PE at a constant temperature.

A particularly interesting data set is from Budrugeac,[32] who reports both isothermal and ramped heating experiments. Of course, the isothermal experiments have initial ramps, and 5−10% of the reaction occurs during those ramps. A rigorous stepwise approach to determine the polymer conversion during ramp-up is detailed further in the mechanistic PE model section. Also, in our regression analysis, that is not a problem, because the analysis integrates through the exact thermal history. Results for a set of models of varying complexity are shown in Table 2. The reaction profile is both narrow and skewed to low temperature, which suggests a single reaction is not adequate. These properties are reflected in the m and n values of the extended Kissinger analysis of the ramped experiments. Optimizing either m or n to all experiments simultaneously to both rates and fractions reacted gave equally good fits. A better fit was obtained by fitting both m and n simultaneously but with a physically unrealistic value of m. A far better fit was obtained using two reactions. The initiation parameter q was 0.99 in all cases.

A comparison of measured and calculated conversion values at ramped and isothermal conditions for the two-reaction model (two independent, parallel, extended Prout−Tompkins reactions, with 15% and 85% relative contributions) is shown in Figure 4. Although the model tends to lag the data a little at the highest conversions for both the ramped and isothermal experiments, the agreement is excellent overall. The two-reaction model is also consistent with the normalized reaction rate plot shown in Figure 5. Above a fraction reacted of 0.2, the data tend to follow an ePT reaction model with $m \approx 0.5$.

Table 2. Extended Prout−Tompkins Kinetic Parameters for HDPE Analyzed by Budrugeac[32]

param	extended Kissinger	m optimized	n optimized	m,n optimized	first reacn = 15%; second reacn = 85%
A_1, s^{-1}	3.92×10^{14}	1.877×10^{15}	9.78×10^{14}	1.600×10^{15}	1.58×10^{9}
E_1, kJ/mol	239.7	247.2	246.0	249.1	161.1
m_1	0.51	0.186	0.000	−0.034	0.000
n_1	0.87	1.00	0.557	0.518	0.826
A_2, s^{-1}					3.46×10^{15}
E_2, kJ/mol					249.0
m_2					0.464
n_2					1.000
r.s.s. of rates		10.2	10.1	3.96	1.18
r.s.s. of conversion		0.91	0.91	0.196	0.098

https://doi.org/10.1021/acs.energyfuels.1c00342
Energy Fuels 2021, 35, 6765−6775

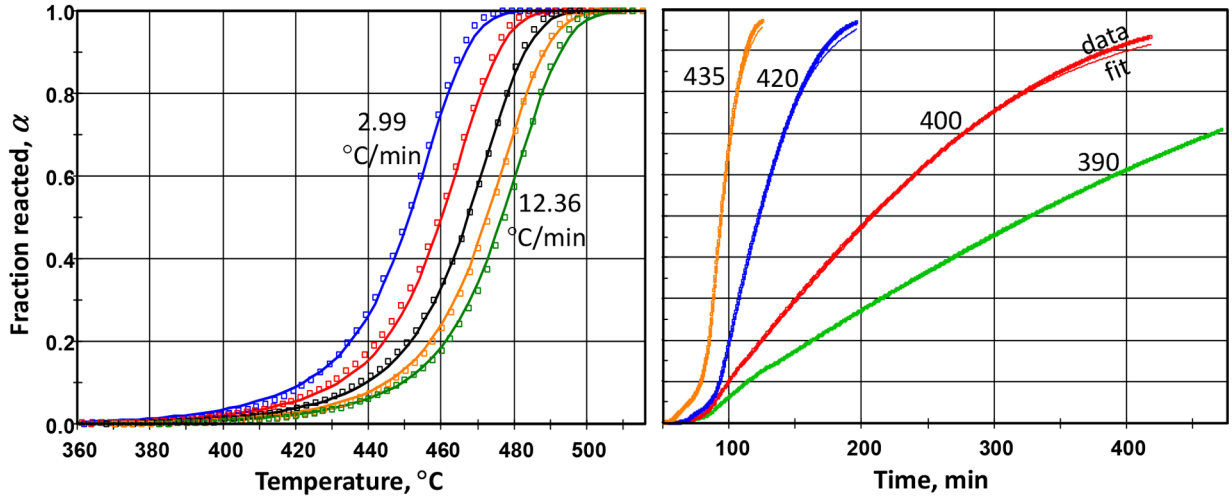

Figure 4. Comparison of calculated conversions (lines) for the two-reaction model in Table 2 with data (points) from Budrugeac[32] at heating rates of 2.99, 4.98, 7.44, 9.88, and 12.36 °C/min and nominally isothermal temperatures from 390 to 435 °C.

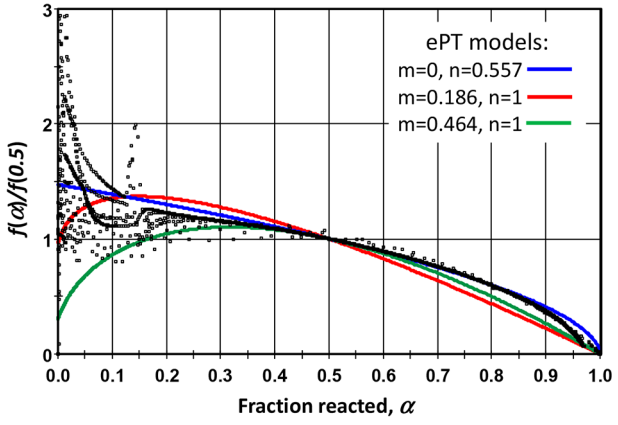

Figure 5. Normalized reaction rate plot for both the ramped and isothermal experiments of Budrugeac.[32] The three colored lines are single-reaction models using parameters from the three nonlinear regression models in Table 2. The anomaly at $\alpha \approx 15\%$ was a momentary thermal excursion in one of the isothermal experiments.

However, at lower conversions, the normalized reaction rate tends to level off and then rise sharply as conversion approaches zero.

Comparing these results with others in the literature, it seems that there is a variable amount of labile material even in nominally high-density PE. The sample analyzed by the Pyromat instrument seems to have the lowest concentration of this labile material, which leads to a sharper reaction profile. The PE used by Budrugeac seems to be typical of commercial HDPE. The temperature of the peak reaction rate of these two materials is very similar.

GLOBAL KINETICS ANALYSIS OF POLYPROPYLENE DECOMPOSITION

Although there are many contributions on the thermal decomposition of PP, an early work by Amorim et al.[20] provides data at both isothermal and ramped heating conditions for 85% isotactic PP. Those data were digitized and analyzed by Kinetics2015 using Friedman isoconversional,[40] Kissinger,[41] and ePT methods. The digitized data were shifted by 5 min to account for reactor heat-up time. The isoconversional results varied somewhat for the different heating regimens, but the general result is that E_a was about 235 kJ/mol over 30−70% conversion and more erratic at high and low conversion, as is typical for that method. Kissinger's method gave E_a = 236 kJ/mol and $A = 5.60 \times 10^{14}$ s^{-1}. The reaction profile was only 63% as wide as a first-order reaction using the Kissinger A and E_a values. The profile asymmetry was 0.68, about the same as a first-order reaction. Using the simple algorithms in Burnham,[18] an initial estimate of m = 0.61 was derived. Subsequent nonlinear regression of the ramped and isothermal data separately and together gave the results in Figure 6, and the resulting kinetic parameters are consistent with the simpler methods. Reaction order n and initiation parameter q were constrained to 1.0 and 0.99, respectively, in all cases. The parameters from fitting all data simultaneously would likely give the most reliable estimate for an arbitrary thermal history.

Figure 7 uses eq 7 to compare all of the data from Amorim et al.[20] to the curves calculated from the ePT parameters derived by nonlinear regression of all data. In addition, Figure 7 shows curves from three other sigmoidal models calculated simply from their functional form.

All models agree qualitatively with the measured results. Each model curve can be changed somewhat by adjusting the relevant shape parameters.[6] For example, changing the random scission chain length, L, from 2 to 8 drops the maximum by 4% and shifts it from 0.25 to 0.28. Similarly, changing the Bouster parameter, b, from 2 to 1.5 decreases the maximum by 5% and shifts it from 0.24 to 0.26. Recall that b has an Arrhenius form, and Bouster et al.[16] found that E_b was negative and b decreased from 2.57 at 331 °C to 1.20 at 380 °C for polystyrene. Amorim et al.[20] found similar values and trends for PP.

The two-parameter ePT model is the most flexible. Changing m to 0.25 shifts the curve maximum to 0.18, and changing it to unity causes the curve to be symmetric about 0.5 conversion. Decreasing n causes the maximum to be shifted to higher conversion, and increasing n causes the opposite shift. Using n = 0.8 causes the normalized rate to agree well for conversion greater than 0.5, but reaction profile width as well as peak shape must be matched, which leads to other parameter constraints.

https://doi.org/10.1021/acs.energyfuels.1c00342
Energy Fuels 2021, 35, 6765−6775

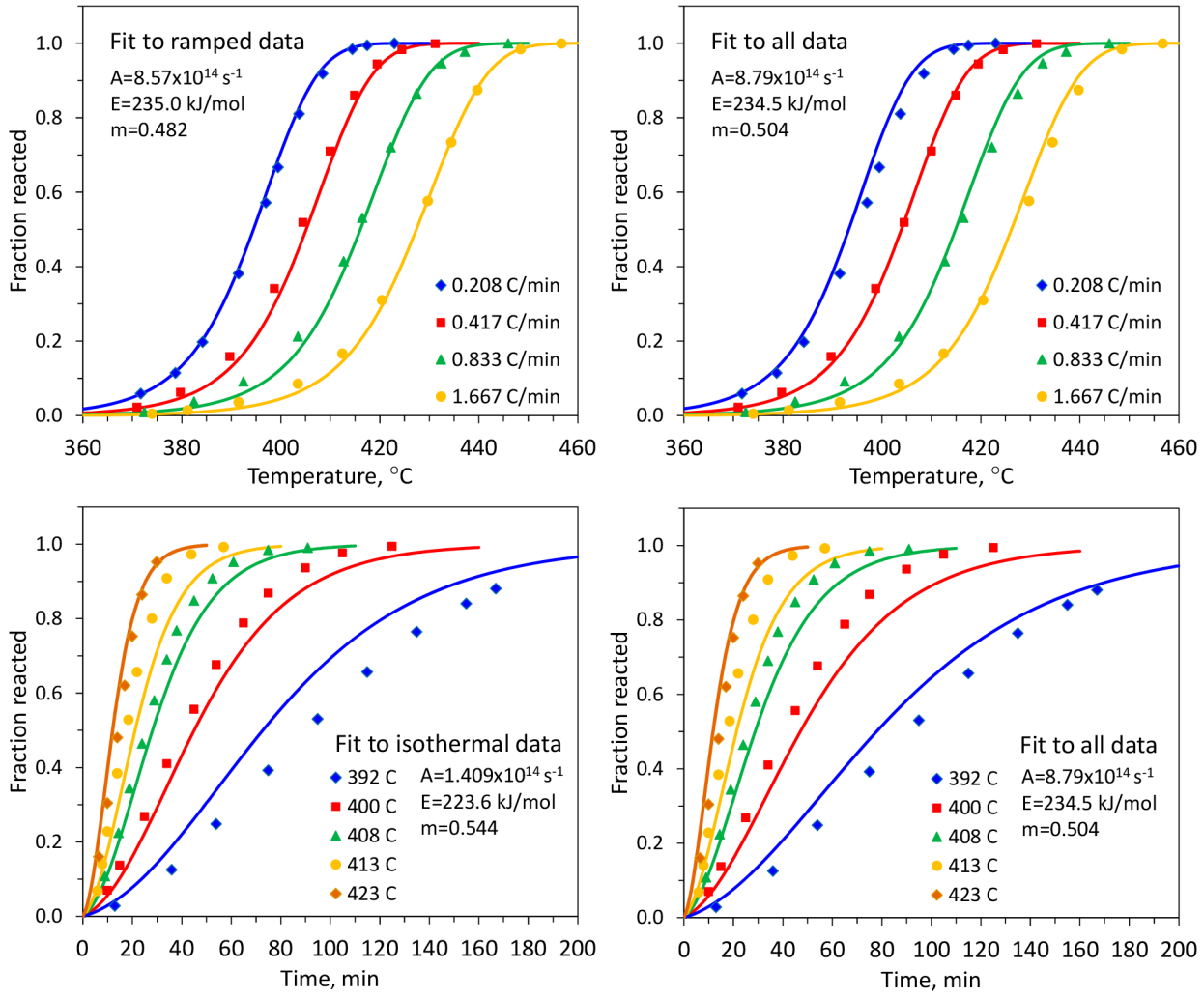

Figure 6. Fits of the ePT model to the PP thermal decomposition data of Amorim et al.[20] Experimental data are shown as points, and fits are depicted using lines.

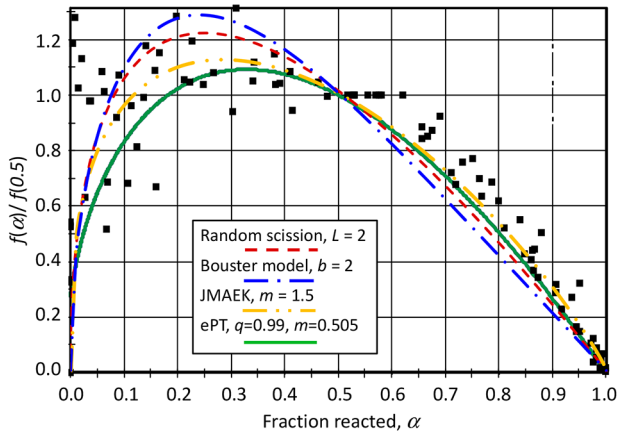

Figure 7. Comparison of observed (points) and calculated (lines) normalized reaction rates, where the former have been calculated for ramped heating using eq 7 from the data of Amorim et al.[20]

MECHANISTIC MODELS

Pyrolysis of polymers, PE and PP in particular, involves a wide variety of reactions leading to a broad product distribution. As mentioned previously, mechanistic models are characterized by detailed reaction mechanisms involving hundreds to thousands of elementary reaction steps and reactive species. Such models allow for detailed product distribution studies based on thermodynamics and kinetics of the underlying reactions, quantifying the short oligomers and small molecules that can be measured experimentally as they are formed from a variety of reaction pathways. It is also possible to track the extent of depolymerization in terms of polymer chain length and molecular weight distribution.

Discrete models based on methods such as kinetic Monte Carlo (kMC) enable tracking of every elementary reaction and the reactant and product species at each time-step. However, it can become complex and computationally intensive to build such models for the pyrolysis of polymers with longer chain lengths. Continuous distribution kinetic models[42,43] involve lumping of polymeric and free-radical species populations that are tracked according to the moments of their distributions and are less computationally expensive. Although the detailed structural information on the degrading polymer is lost, these models can still provide its molecular weight distribution and structural detail at the level of the types of chains that are tracked (e.g., chains with unsaturated groups, chains with weak links, and so on). Vinu and Broadbelt,[44] and Zhou, Broadbelt, and Vinu[45] presented a detailed overview of the continuum

https://doi.org/10.1021/acs.energyfuels.1c00342
Energy Fuels 2021, 35, 6765−6775

Table 3. Reaction Family Parameters Used in Mechanistic Models of PE and PP[a]

reacn type	A (s^{-1} or L mol^{-1} s^{-1})[b]	E_0[c] (kcal mol^{-1})	γ[d]	representative ΔH_{reacn}(kcal/mol) for HDPE
chain fission	1.00×10^{16}	2.3	1	87.4
allyl chain fission	5.50×10^{13}	2.3	1	72.9
radical recombination	1.10×10^{11}	2.3	0	−87.4
disproportionation	1.10×10^{10}	2.3	0	-
end-chain β-scission	1.29×10^{13}	11.4	0.76	22.3
mid-chain β-scission	5.35×10^{14}	11.4	0.76	23.0
	8.00×10^{14}			
β-scission to LMWS	2.33×10^{13}	11.4	0.76	22.0
	8.00×10^{14}			
radical addition	2.88×10^{7}	11.4	0.24	−23.0
hydrogen abstraction	2.75×10^{8}	12.0		−1.57
	5.00×10^{8}			
1,4-hydrogen shift	1.58×10^{11}			
1,5-hydrogen shift	1.82×10^{10}			
1,6-hydrogen shift	1.05×10^{10}			
1,7-hydrogen shift	3.00×10^{9}			
$x,x+$ 3-hydrogen shift	1.00×10^{11}			
$x,x+$ 4-hydrogen shift	1.26×10^{10}			
$x,x+$ 5-hydrogen shift	7.24×10^{9}			

[a]Boldfaced values are adjusted in this work. Rate parameters are taken from Levine and Broadbelt.[14] [b]A = frequency factor. [c]E_0 = intrinsic barrier. [d]γ = transfer coefficient.

models for polymer pyrolysis. In brief, the population balance rate equations are solved by applying the method of moments to determine the concentration, mean, and spread of similar polymer species that are grouped by specific features but not their chain length, which is tracked as distributions according to moments. The details of the model formulation, rules used for the different reaction families in the generalized mechanism above, and other specific details are outlined in the reviews.[43,44]

While the diversity of reactions and the level of detail that is tracked in mechanistic models are its strengths, they present challenges because a rate coefficient needs to be specified for each distinct reaction in the model. Therefore, a hierarchical approach to specifying rate coefficients is used, leveraging structure−reactivity relationships. The Evans−Polanyi kinetic correlation,[46] given as $E_a = E_0 + \gamma \times \Delta H_{reacn}$, specifies the activation energy of individual reactions from the enthalpy of reaction and two reaction family parameters, E_0 and γ, an intrinsic barrier and transfer coefficient, respectively. In addition, each reaction in a reaction family shares the same Arrhenius pre-exponential factor. Using these correlations, temperature-dependent rate coefficients can be calculated using the Arrhenius equation, $k = A \times \exp(-E_a/RT)$. The combination of the mechanistic formulation of the reactions and their rate coefficients with reactor design equations that describe the reactor of interest allows for the interrogation of reaction pathways at the mechanistic level.

MECHANISTIC ANALYSIS OF POLYETHYLENE DECOMPOSITION

The model developed by Levine and Broadbelt[14] was employed to obtain mechanistic insights into PE pyrolysis. The reaction family parameters in the model of Levine and Broadbelt are summarized in Table 3. The model was used to simulate the experimental data of Westerhout et al.,[27] corresponding to isothermal HDPE pyrolysis at 440 °C. When the model parameters were used without adjustment, the overall rates compared to the experimental data were slightly low. Given that the pre-exponential factors are representative values, it is feasible to adjust them slightly within the bounds set by transition-state theory, particularly since Levine and Broadbelt developed their model against data collected in closed batch reactors in which secondary or tertiary reactions may be more prevalent. Specifically, $A_{H\text{-}abs}$ and $A_{\beta\text{-}scission}$ were selected for slight adjustment. In general, $A_{H\text{-}abs}$ increased the initial rate of conversion of PE, while an increase in $A_{\beta\text{-}scission}$ increased the overall conversion. Moreover, higher $A_{H\text{-}abs}$ values significantly lowered the end-chain radical concentrations and led to a faster production of low molecular weight (LMW) radical species. On the other hand, higher β-scission rates increased the concentration of these LMW radical species, which explains the increase in overall conversion. The final values of $A_{H\text{-}abs}$ and $A_{\beta\text{-}scission}$ adjusted against the data of Westerhout et al.[27] are summarized in Table 3.

The model with the rate parameters validated against the data of Westerhout and co-workers was then used without any further adjustment in parameters to predict a different data set, the experimental data reported by Budrugeac[32] under quasi-isothermal conditions (Figure 8). The model simulations were performed with a stepwise temperature profile that mimics the quasi-isothermal temperature profile. It can be observed from Figure 8 that there was negligible conversion predicted by the model during the temperature ramp, which is in good agreement with Budrugeac's data. The overall trends in the temperature dependence are captured very well, with a slight underproduction of the rate at the lowest temperature and times. Notably, though, the sigmoidal character of PE pyrolysis is clearly observed, manifesting at temperatures as low as 400 °C and persisting even at higher temperatures.

The detail inherent in the mechanistic model allows a quantitative analysis of the observed sigmoidal character. Kinetic chain length, calculated as the ratio of the rate of radical propagation to the rate of initiation, is shown for PE in Figure 9 for a wide range of pyrolysis temperatures. The longer the kinetic chain length, the longer a free radical can react

https://doi.org/10.1021/acs.energyfuels.1c00342
Energy Fuels 2021, 35, 6765−6775

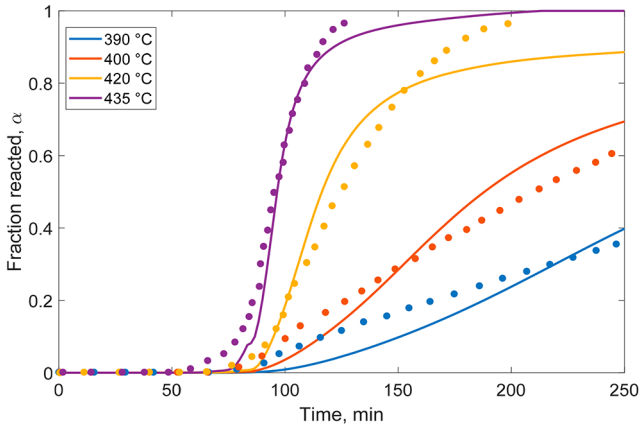

Figure 8. Comparison of predictions of conversion from the HDPE mechanistic model (lines) and the experimental data reported by Budrugeac.[32]

before terminating. The sigmoidal decomposition of PE stems from the slower rate of radical initiation relative to the dominating rate of propagation comprised of an accumulation of more-stable mid-chain and primary end-chain carbon radicals, thus accelerating the conversion of the polymer fraction to LMW products. Additionally, as the temperature increases, the rate of initiation has a stronger temperature dependence (higher E_a) and increases more than that of propagation, thus lowering the ratio and shortening the chain length. Although the detail is not shown here, it is important to note that the rate of initiation and the rate of propagation are not simply a result of one reaction each but instead are calculated from the rates of tens to hundreds of individual elementary steps. Thus, the overall rates represented in Figure 9 as a single kinetic chain length changing as a function of time and temperature can be dissected in even greater detail if desired, allowing the dominant rates of each family to be identified and related to the specific radical classes or chain types that are contributing most significantly. Furthermore, the evolution of individual low molecular weight products is also explicitly provided by the model. Results are not shown here since the focus of this work is on conversion and global conversion measures, but temporal yields of products as a function of time and temperature are output by the model.

MECHANISTIC ANALYSIS OF POLYPROPYLENE DECOMPOSITION

The global analysis of PP decomposition kinetics revealed interesting differences in the rate signatures for isotactic versus atactic PP. The orientation of methyl groups along the backbone of PP impacts the crystallinity of the polymer on the macroscale. Isotactic or semicrystalline polypropylene (IPP) has regular order in that the pendant methyl groups are aligned, whereas atactic or amorphous polypropylene (APP) has a random steric structure.[47] Translating the physical structure to chemical behavior, IPP has clearly sigmoidal isothermal conversion, just as HDPE does. However, APP has a deceleratory decomposition rate, as demonstrated by Amorim et al.[20]

To isolate the effects of chemical structure and physical influences, polypropylene decomposition was studied in silico by using the PE mechanistic model and accounting for the difference that -[CH_2−$CH(CH_3)$]- repeat units in PP compared to -[CH_2− CH_2]- repeat units in PE would have on the intrinsic kinetics. That is, the introduction of branched carbon atoms influences bond strengths and the heats of reaction for the elementary steps underlying the mechanistic model, and thus, the same reactions in PE and PP all naturally have different rate coefficients, influencing the relative rates of all of the reactions in the model. Following the methods of Kruse et al.[12] who built a comprehensive PP pyrolysis model, the reaction family parameters (pre-exponential factors and Evans−Polanyi parameters) from the HDPE model were used without adjustment, but the heats of reaction for individual reactions were calculated on the basis of the structure of the species specifically contained in the PP model. As seen in Figure 10, the variation of reaction rate with conversion of PP is noticeably deceleratory. This behavior is a hallmark of APP

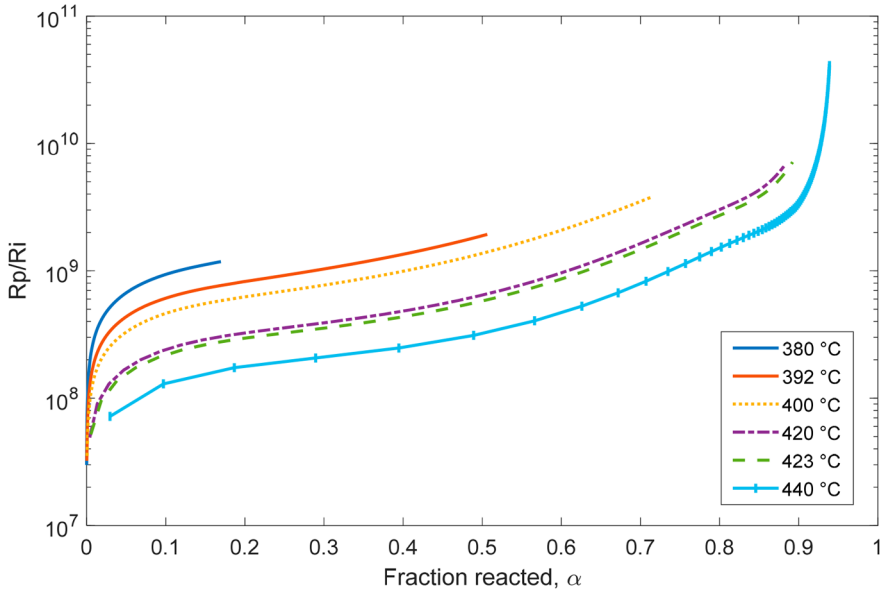

Figure 9. Variation in HDPE kinetic chain length, R_p/R_i, as a function of fraction reacted at temperatures over the range of 380−440 °C.

https://doi.org/10.1021/acs.energyfuels.1c00342
Energy Fuels 2021, 35, 6765−6775

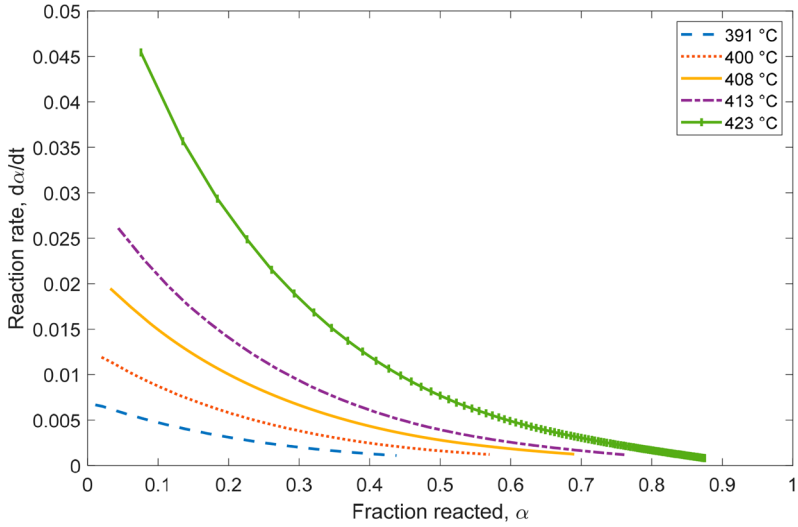

Figure 10. Predictions from the mechanistic model of variation of the reaction rate, $d\alpha/dt$, of PP decomposition as a function of fraction reacted, α.

as noted above and is in sharp contrast to the IPP pyrolysis behavior in Figure 6.

The mechanistic model is agnostic to tacticity and takes into account the difference between HDPE and PP based on monomeric structural differences alone as captured in differences in enthalpies of reaction. For radical initiation via chain fission, PP has a higher rate constant than HDPE due to the lower enthalpy of reaction and, consequentially, the lower activation energy. However, both polymers have approximately the same rate of radical propagation, so HDPE has an overall longer kinetic chain that results in higher reactivity over time as radical concentration accumulates. PP appears to become less reactive as it degrades due to the initial high rate of radical formation from chain fission, lowering the ratio of propagation to initiation. This may be a matter of degree, such that the PP pyrolyzed in this model has unhindered radical initiation via bond fission, thus lowering this kinetic chain length. This suggests that further effects from structural differences such as tacticity manifest independently from differences in the structure of the backbone monomers, resulting in distinct variations in observed reaction kinetics. By controlling for one of these factors, the effect of chemical structure alone was identified and shown to be profound. This result also suggests that taking physical differences imparted by tacticity (i.e., IPP versus APP) into account would be important. Chen and co-workers[48] also highlight the importance of intermolecular effects such as chain mobility and viscosity on the apparent activation energy, where isotactic polystyrene has an enhanced thermal stability relative to atactic polystyrene. A similar phenomenon may be at play with PP, where APP has a lower viscosity and thus greater chain mobility compared to IPP, thus increasing the rate of radical diffusion and propagation throughout the melt sample.

While a global model can easily be fit to capture these differences, they do not provide the insight offered here by the mechanistic foundation of the more detailed model based on monomer identity, backbone composition, and elementary steps. Additionally, the purity of the literature samples used are unknown. It is possible that remnants of polymerization catalysts or oxygen are present in the polymer, especially for PP, which is highly sensitive to oxidation, particularly in the amorphous phase.[49] Kruse and co-workers[12] included weak peroxide links to mimic structural defects in a modified version of the PP model used here to accelerate radical initiation and found that weak-link fission does increase the rate of radical initiation, but at temperatures above 350 °C carbon−carbon bond fission dominates. More detailed models could include further oxidative degradation,[50] such as reactions found in the autoxidation of condensed-phase hydrocarbons.[51,52]

CONCLUSIONS

Isothermal and ramped thermal analysis of PE and PP are modeled with global, lumped, and mechanistic methods. Lumped and global models can capture experimental results with strong agreement, but mechanistic models offer insight into the effect of structural characteristics on the intrinsic kinetics of polyolefin pyrolysis. Detailed analysis of relative rates of reaction of tens to hundreds of elementary steps can be used to understand the origin of macroscopic measures such as sigmoidal character of the conversion as a function of time. The mechanistic model was able to toggle this behavior by modifying only the monomer structure of the polymeric backbone and its attendant effect on the rate coefficients through heats of reaction for individual elementary steps. This analysis shows that other characteristics such as tacticity would need to be layered on top of these chemical structural effects, which may be best incorporated with kMC, which tracks individual chains and even can account for spatial effects. The results from studying PE and PP here fall in the expected trend of polyolefins from HDPE to LDPE to PP regarding backbone branching and effects.

A final note is that while the mechanistic models provide detailed product information, it was not given here because it is difficult to harmonize thermal analysis and product measurements with the required detail for comparison to the model. Thus, the authors encourage future experiments to collect high-quality kinetic data and measure product yields in the same experiments. For example, the pyrolysis of HDPE has hundreds of products, and mechanistic models are inherently compatible with this level of detail, so it would be useful to do thermogravimetric analysis with detailed product analysis.

https://doi.org/10.1021/acs.energyfuels.1c00342
Energy Fuels 2021, 35, 6765−6775

AUTHOR INFORMATION

Corresponding Author

Alan K. Burnham − *Alan Burnham Consultant, Livermore, California 94550, United States;* orcid.org/0000-0002-3101-4419; Email: akburnham@yahoo.com

Authors

Rebecca E. Harmon − *Department of Chemical and Biological Engineering, Northwestern University, Evanston, Illinois 60208, United States; Van't Hoff Institute for Molecular Sciences, University of Amsterdam, Amsterdam 1098, XH, The Netherlands;* orcid.org/0000-0003-1549-7446

Gorugantu SriBala − *Department of Chemical and Biological Engineering, Northwestern University, Evanston, Illinois 60208, United States;* orcid.org/0000-0001-8624-2251

Linda J. Broadbelt − *Department of Chemical and Biological Engineering, Northwestern University, Evanston, Illinois 60208, United States;* orcid.org/0000-0003-4253-592X

Complete contact information is available at: https://pubs.acs.org/10.1021/acs.energyfuels.1c00342

Notes

The authors declare no competing financial interest.

ACKNOWLEDGMENTS

This material is based in part upon work supported by the U.S. Department of Energy's Office of Energy Efficiency and Renewable Energy (EERE) under the Bioenergy Technologies Office Award No. DE-EE0008928. Support of the Institute for Sustainability and Energy (ISEN) at Northwestern University is gratefully acknowledged. Financial support from the National Science Foundation (NSF) Partnerships for International Research and Education (PIRE) program under Grant No. 1743748 is also gratefully acknowledged. We thank Dr. Budrugeac for providing his data for our analysis. We also thank Dr. Seth Levine and Dr. Pavlo Kostetskyy for their assistance in mechanistic model troubleshooting.

REFERENCES

(1) Ragaert, K.; Delva, L.; Van Geem, K. Mechanical and chemical recycling of solid plastic waste. *Waste Manage.* **2017**, *69*, 24−58.

(2) Saptoadi, H.; Pratama, N. N. Utilization of plastics waste oil as partial substitute for kerosene in pressurized cookstoves. *Int. J. Environ. Sci. Dev.* **2015**, *6* (5), 363−368.

(3) Burnham, A. K.; Braun, R. L.; Coburn, T. T.; Sandvik, E. I.; Curry, D. J.; Schmidt, B. J.; Noble, R. A. An appropriate kinetic model for well-preserved algal kerogens. *Energy Fuels* **1996**, *10*, 49−59.

(4) Braun, R. L.; Burnham, A. K.; Reynolds, J. G.; Clarkson, J. E. Pyrolysis kinetics for lacustrine and marine source rocks by programmed micropyrolysis. *Energy Fuels* **1991**, *5* (1), 192−204.

(5) Burnham, A. K. *Global Chemical Kinetics of Fossil Fuels*; Springer: Cham, Switzerland, 2017; chapters 5−7, DOI: 10.1007/978-3-319-49634-4_5.

(6) Burnham, A. K.; Zhou, X.; Broadbelt, L. J. Critical review of the global chemical kinetics of cellulose thermal decomposition. *Energy Fuels* **2015**, *29* (5), 2906−2918.

(7) Klein, M. T.; Neurock, M.; Broadbelt, L.; Foley, H. C. Reaction pathway analysis. In *Selectivity in Catalysis*; ACS Symposium Series; American Chemical Society, 1993; Vol. *517*, pp 290−312, DOI: 10.1021/bk-1993-0517.ch020.

(8) Rice, F. O. The thermal decomposition of organic compounds from the standpoint of free radicals. I. Saturated compounds. *J. Am. Chem. Soc.* **1931**, *53* (5), 1959−1972.

(9) Rice, F. O.; Herzfeld, K. F. The thermal decomposition of organic compounds from the standpoint of free radicals. VI. The mechanism of some chain reactions. *J. Am. Chem. Soc.* **1934**, *56* (2), 284−289.

(10) National Bureau of Standards (NBS) *Polymer Degradation Mechanisms*, NBS Circular No. 525; NBS, U.S. Department of Commerce, 1953; pp 1−280.

(11) De Witt, M. J.; Dooling, D. J.; Broadbelt, L. J. Computer generation of reaction mechanisms using quantitative rate information: Application to long-chain hydrocarbon pyrolysis. *Ind. Eng. Chem. Res.* **2000**, *39* (7), 2228−2237.

(12) Kruse, T. M.; Wong, H.-W.; Broadbelt, L. J. Mechanistic modeling of polymer pyrolysis: Polypropylene. *Macromolecules* **2003**, *36* (25), 9594−9607.

(13) Kruse, T. M.; Levine, S. E.; Wong, H.-W.; Duoss, E.; Lebovitz, A. H.; Torkelson, J. M.; Broadbelt, L. J. Binary mixture pyrolysis of polypropylene and polystyrene: A modeling and experimental study. *J. Anal. Appl. Pyrolysis* **2005**, *73* (2), 342−354.

(14) Levine, S. E.; Broadbelt, L. J. Detailed mechanistic modeling of high-density polyethylene pyrolysis: Low molecular weight product evolution. *Polym. Degrad. Stab.* **2009**, *94* (5), 810−822.

(15) Simha, R.; Wall, L. A. Kinetics of chain depolymerization. *J. Phys. Chem.* **1952**, *56* (6), 707−715.

(16) Bouster, C.; Vermande, P.; Veron, J. Study of the pyrolysis of polystyrenes: I. Kinetics of thermal decomposition. *J. Anal. Appl. Pyrolysis* **1980**, *1* (4), 297−313.

(17) Prout, E. G.; Tompkins, F. C. The thermal decomposition of silver permanganate. *Trans. Faraday Soc.* **1946**, *42* (0), 468−472.

(18) Burnham, A. K. Application of the Šesták-Berggren equation to organic and inorganic materials of practical interest. *J. Therm. Anal. Calorim.* **2000**, *60* (3), 895−908.

(19) Sánchez-Jiménez, P. E.; Pérez-Maqueda, L. A.; Perejón, A.; Criado, J. M. A new model for the kinetic analysis of thermal degradation of polymers driven by random scission. *Polym. Degrad. Stab.* **2010**, *95* (5), 733−739.

(20) Sousa Pessoa De Amorim, M. T.; Bouster, C.; Veron, J. Pyrolysis of polypropylene: II. Kinetics of degradation. *J. Anal. Appl. Pyrolysis* **1982**, *4* (2), 103−115.

(21) Johnson, W. A.; Mehl, R. F. Reaction kinetics in processes of nucleation and growth. *Trans. Am. Inst. Mining Met. Eng.* **1939**, *135*, 733−739.

(22) Avrami, M. Kinetics of phase change. II Transformation-time relations for random distribution of nuclei. *J. Chem. Phys.* **1940**, *8* (2), 212−224.

(23) Erofe'ev, B. V. C. R. Generalized equation of chemical kinetics and its application to reactions involving solids. *Dokl. Akad. Sci, USSR* **1946**, *52*, 511−514.

(24) Kolmogorov, A. A statistical theory for the recrystallization of metals. *Izv. Akad. Nauk USSR Neorg. Mater.* **1937**, *1*, 355−359.

(25) Burnham, A. K.; Weese, R. K.; Wemhoff, A. P.; Maienschein, J. L. A historical and current perspective on predicting thermal cookoff behavior. *J. Therm. Anal. Calorim.* **2007**, *89* (2), 407−415.

(26) Flynn, J. H.; Florin, R. E. Degradation and pyrolysis mechanisms. In *Pyrolysis and GC in Polymer Analysis*; Liebman, S. A., Levy, E. J., Eds.; Marcel Dekker: New York, 1985; pp 149−208.

(27) Westerhout, R. W. J.; Waanders, J.; Kuipers, J. A. M.; van Swaaij, W. P. M. Kinetics of the low-temperature pyrolysis of polyethene, polypropene, and polystyrene modeling, experimental determination, and comparison with literature models and data. *Ind. Eng. Chem. Res.* **1997**, *36* (6), 1955−1964.

(28) Burnham, A. K.; Braun, R. L. Global kinetic analysis of complex materials. *Energy Fuels* **1999**, *13* (1), 1−22.

(29) Peterson, J. D.; Vyazovkin, S.; Wight, C. A. Kinetics of the thermal and thermo-oxidative degradation of polystyrene, polyethylene and poly(propylene). *Macromol. Chem. Phys.* **2001**, *202* (6), 775−784.

(30) Gotor, F. J.; Criado, J. M.; Malek, J.; Koga, N. Kinetic analysis of solid-state reactions: The universality of master plots for analyzing

isothermal and nonisothermal experiments. *J. Phys. Chem. A* **2000**, *104* (46), 10777−10782.
(31) Vyazovkin, S. Kissinger method in kinetics of materials: Things to beware and be aware of. *Molecules* **2020**, *25*, 2813.
(32) Budrugeac, P. Theory and practice in the thermoanalytical kinetics of complex processes: Application for the isothermal and non-isothermal thermal degradation of HDPE. *Thermochim. Acta* **2010**, *500* (1), 30−37.
(33) u, C.-H.; Chang, C.-Y.; Hor, J.-L.; Shih, S.-M.; Chen, L.-W.; Chang, F.-W. On the thermal treatment of plastic mixtures of MSW: Pyrolysis kinetics. *Waste Manage.* **1993**, *13* (3), 221−235.
(34) Albano, C.; de Freitas, E. Thermogravimetric evaluation of the kinetics of decomposition of polyolefin blends. *Polym. Degrad. Stab.* **1998**, *61* (2), 289−295.
(35) Kim, S.; Jang, E.-S.; Shin, D.-H.; Lee, K.-H. Using peak properties of a DTG curve to estimate the kinetic parameters of the pyrolysis reaction: Application to high density polyethylene. *Polym. Degrad. Stab.* **2004**, *85* (2), 799−805.
(36) Kayacan, İ.; Doğan, Ö. M. Pyrolysis of low and high density polyethylene. Part I: Non-isothermal pyrolysis kinetics. *Energy Sources, Part A* **2008**, *30* (5), 385−391.
(37) Aboulkas, A.; El harfi, K.; El Bouadili, A. Thermal degradation behaviors of polyethylene and polypropylene. Part I: Pyrolysis kinetics and mechanisms. *Energy Convers. Manage.* **2010**, *51* (7), 1363−1369.
(38) Das, P.; Tiwari, P. Thermal degradation kinetics of plastics and model selection. *Thermochim. Acta* **2017**, *654*, 191−202.
(39) Dubdub, I.; Al-Yaari, M. Pyrolysis of low density polyethylene: Kinetic study using TGA data and ANN prediction. *Polymers* **2020**, *12*, 891.
(40) Friedman, H. L. Kinetics of thermal degradation of char-forming plastics from thermogravimetry. Application to a phenolic plastic. *J. Polym. Sci., Part C: Polym. Symp.* **1964**, *6* (1), 183−195.
(41) Kissinger, H. E. Reaction kinetics in differential thermal analysis. *Anal. Chem.* **1957**, *29* (11), 1702−1706.
(42) Madras, G.; McCoy, B. J. Distribution kinetics for polymer mixture degradation. *Ind. Eng. Chem. Res.* **1999**, *38* (2), 352−357.
(43) Madras, G.; Smith, J. M.; McCoy, B. J. Degradation of poly(methyl methacrylate) in solution. *Ind. Eng. Chem. Res.* **1996**, *35* (6), 1795−1800.
(44) Vinu, R.; Broadbelt, L. J. Unraveling reaction pathways and specifying reaction kinetics for complex systems. *Annu. Rev. Chem. Biomol. Eng.* **2012**, *3* (1), 29−54.
(45) Zhou, X.; Broadbelt, L. J.; Vinu, R. Mechanistic understanding of thermochemical conversion of polymers and lignocellulosic biomass. *Adv. Chem. Eng.* **2016**, *49*, 95−198.
(46) Evans, M. G.; Polanyi, M. Inertia and driving force of chemical reactions. *Trans. Faraday Soc.* **1938**, *34* (0), 11−24.
(47) Natta, G.; Corradini, P. Structure and properties of isotactic polypropylene. In *Stereoregular Polymers and Stereospecific Polymerizations*; Natta, G., Danusso, F. B. T., Eds.; Pergamon, 1967; pp 743−746, DOI: 10.1016/B978-1-4831-9882-8.50057-9Ge.
(48) Chen, K.; Harris, K.; Vyazovkin, S. Tacticity as a factor contributing to the thermal stability of polystyrene. *Macromol. Chem. Phys.* **2007**, *208* (23), 2525−2532.
(49) Knight, J. B.; Calvert, P. D.; Billingham, N. C. Localization of oxidation in polypropylene. *Polymer* **1985**, *26* (11), 1713−1718.
(50) Ryan, T. G.; Calvert, P. D.; Billingham, N. C. The distribution of additives and impurities in isotactic polypropylene. In *Stabilization and Degradation of Polymers*; Advances in Chemistry; American Chemical Society, 1978; Vol. *169*, pp 22−261, DOI: 10.1021/ba-1978-0169.ch022.
(51) Pfaendtner, J.; Broadbelt, L. J. Mechanistic modeling of lubricant degradation. II. The autoxidation of decane and octane. *Ind. Eng. Chem. Res.* **2008**, *47* (9), 2897−2904.
(52) Orlova, Y.; Harmon, R. E.; Broadbelt, L. J.; Iedema, P. D. Review of the kinetics and simulations of linseed oil autoxidation. *Prog. Org. Coat.* **2021**, *151*, 106041.

https://doi.org/10.1021/acs.energyfuels.1c00342
Energy Fuels 2021, 35, 6765−6775